Radiative Metallic Thermal Protection Systems: A Status Report

Herman L. Bohon,* John L. Shideler,† and Donald R. Rummler‡
NASA Langley Research Center, Hampton, Va.

During the early stages of the space shuttle program, there were a number of technological uncertainties concerning the applicability of metallic thermal protection systems (TPS) to the multimission environment of the shuttle. To resolve the uncertainties and to advance the state-of-the-art, a broad-based technology program was initiated to develop metallic TPS over the temperature range from 810 to 1590 K. Wind-tunnel tests, conducted to assess the influence of surface/stream interaction of wavy surfaces on the design of metallic TPS, indicate small increases in heat flux and surface drag for flow angles less than 20 deg. Analytical and experimental investigations, recently completed, have improved prediction methods significantly for cyclic creep behavior of TPS components repeatedly exposed to complex mission cycles. Thermal/structural concept optimization studies to minimize mass while maintaining structural integrity have led to advanced designs with unit masses which are competitive with those for shuttle reusable surface insulation (RSI). In addition, the durability and reusability of metallic TPS have been demonstrated repeatedly in tests of full-scale systems. The current state-of-the-art strongly suggests that radiative metallic TPS have come of age.

Nomenclature

C_d = drag coefficient
C_p = pressure coefficient
H_T = enthalpy
h = heat-transfer coefficient
M = Mach number
P = pressure
P_T = total pressure
P_s = static pressure
q = dynamic pressure
R_e = Reynolds number
T = temperature
t = time
δ = boundary-layer thickness
Λ = yaw angle

Introduction

IF utilization of near-Earth space is to become routine, advanced space transportation systems must become fully reusable and have longer life, lower operating cost, and greater operational flexibility than the current space shuttle system.[1,2] Mission requirements envisioned for the 1990's and beyond range from highly maneuverable, single-stage-to-orbit, lifting-entry vehicles to reusable ballistic-entry vehicles. Payload capability may be as low as 2720 kg for the maneuverable vehicles and up to 272,000 kg for the ballistic vehicles. A key factor in the reusability, life, and operational flexibility of such classes of vehicles is the thermal protection system (TPS).

The current space shuttle TPS, reusable surface insulation (RSI), is inherently fragile and, consequently, its reusability may not be sufficient for advanced mission requirements. Radiative metallic TPS, on the other hand, are generically nonfragile and reusable. However, during the early stages of the space shuttle program, there were a number of technological uncertainties concerning the applicability of metallic thermal protection systems to the multimission environment of the shuttle.[3] To resolve the uncertainties and to advance the state-of-the-art, a broad-based technology program was initiated to develop metallic TPS over the temperature range from 810 to 1590 K. Within this program, large metallic TPS designs have been designated and fabricated, and tests in simulated entry environments have demonstrated thermal and structural performance potentials. Specific research programs have registered significant progress in several areas, such as determination of the influence of wavy surfaces on pressure drag and localized heating, improvements in cyclic creep predictions for several candidate TPS materials in complex load environments, thermal/structural optimization to achieve minimum weight while maintaining thermal and structural integrity, and performance demonstration of metallic TPS through tests and analysis.

Although the TPS programs have been focused on requirements of the space shuttle, the technology developed is applicable to advanced space transports and hypersonic cruise vehicles. This paper addresses the status of radiative metallic TPS as it has evolved during the technology program and reviews current research activity to assess durability and service life of advanced TPS designs.

Metallic Thermal Protection System

General Features

The major features of a metallic TPS are shown in Fig. 1. The TPS consists of the radiative surface panel, the supports, and insulation package. As indicated in Fig. 1, the radiative surface is typically corrugated. The wavy surface provides relatively free thermal growth transverse to the corrugations and provides stiffness to resist bending loads due to surface pressure and to resist panel flutter. Flexible supports are designed to accommodate longitudinal thermal expansion while retaining sufficient stiffness to transmit surface pressure loads to the primary structure. Also prominent in metallic TPS designs are expansion joints, which must absorb longitudinal thermal growth of the radiative surface and simultaneously prevent the ingress of hot boundary-layer gases to the panel interior. The insulation consists of flexible

Received March 17, 1977; presented as Paper 77-391 at the AIAA/ASME 18th Structures, Structural Dynamics, and Materials Conference, San Diego, Calif., March 21-23, 1977 (in bound Vol. A of Conference papers); revision received June 9, 1977.
Index categories: Structural Design; Thermal Control.

*Aerospace Engineer, Thermal Structures Branch, Structures and Dynamics Division. Member AIAA.
†Aerospace Engineer, Thermal Structures Branch, Structures and Dynamics Division.
‡Materials Engineer, Materials Research Branch, Materials Division.

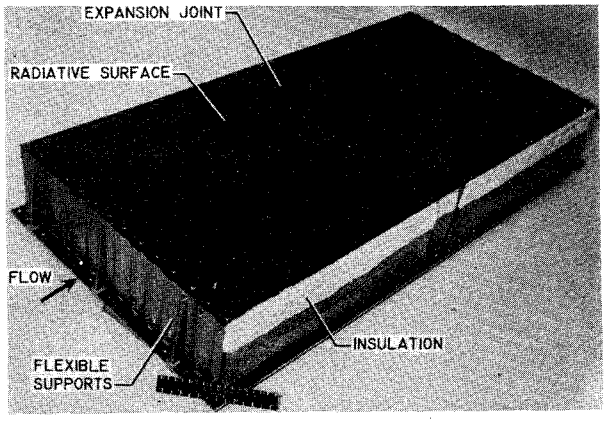

Fig. 1 Typical metallic thermal protection system.

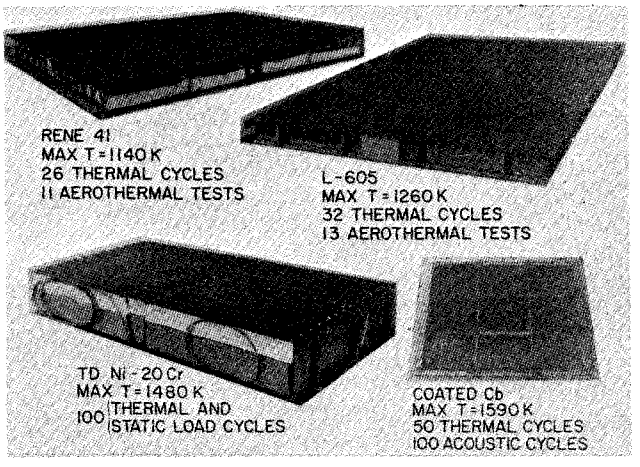

Fig. 2 Radiative metallic TPS test models.

thermal blankets often encapsulated in foil material to prevent moisture absorption. The insulation must protect the primary load-carrying structure from the high external temperatures.

Technology Uncertainties

The TPS of the current space shuttle has a 100-mission life requirement, and recent studies[2] indicate that future space transports may require a life of up to 500 missions to obtain the national goal of economical exploitation of space. The capability of metallic TPS to meet these requirements depends upon the resolution of several technology uncertainties. For example, the thermal protection system must have sufficient durability and reusability in order to withstand repeated exposure to the adverse environments of launch, space, and re-entry, as well as the abuse due to normal ground maintenance. Because of the wavy surface designs of metallic TPS, an assessment of surface/stream interaction effects to determine surface drag and heating penalties is required. In addition, with the requirement for greater reusability, cyclic creep becomes an increasing concern. Design improvements aimed at reducing unit masses over those of early shuttle metallic TPS concepts are desired. Finally, the demonstration of TPS reusability and cyclic life requires unique ground facilities that can simulate the adverse environment of Earth entry. Recent technology advancements in each of the preceding areas are discussed in the following sections.

Durability and Reusability

A measure of the toughness of metallic TPS has been provided through mission cycle tests of various candidate models. Table 1 lists an array of flight-weight TPS test articles designed and fabricated under the technology program at Langley for evaluation in various sequential and/or combined test environments.[4-9] The articles listed include current state-of-the-art designs, as well as advanced thermal-structural designs. With the exception of the coated columbium concept, design types are predominantly corrugation-stiffened with either convex or concave surfaces. The fabricated panels were sized to mate with available test fixtures, but all designs included multiple bays in order to assess potential expansion joint problems. The unit masses tabulated include all component parts exterior to the primary structure, that is, panel, supports, insulation, and attachment hardware. As can be seen from the table, the TPS hardware are in various stages of testing.

Four of the large flight-weight models which have demonstrated durability of metallic TPS are shown in Fig. 2. The top two configurations of René 41 (nickel base) and L-605 (cobalt base) were subjected to 26 and 32 simulated Earth entry thermal cycles, respectively, using radiant heat lamps. During several of these tests, the heated panels were inserted rapidly into an aerodynamic stream to impose boundary-layer flow conditions representative of those for a prescribed point in the entry cycle.[4,5] These aerothermal tests were conducted in the Mach 7 stream of the Langley 8-ft high-temperature structures tunnel (HTST) and imposed true aerodynamic heating to the surfaces, as well as differential pressures representative of entry conditions. The aerothermal tests also demonstrated that simple expansion joints will prevent the flow of hot boundary-layer gases to the panel interior. When tests on these two panels were terminated, they were in excellent condition after multiple mission cycles and had shown no evidence of thermal or structural degradation.

The TD Ni-20Cr panel was tested statically at Grumman Aerospace Corporation for 100 cycles of ascent pressure loads (up to 20 kPa) and combined entry thermal and pressure loads.[6] The pressure loads were applied to the model by an array of loading wires attached at 84 discrete points on the front face. The wires penetrated the insulation blanket and were attached to a whiffle-tree loading device. During the 100 mission cycles, the only observed damage to the model was six surface cracks, each located at discrete load points. Nevertheless, the panel continued to sustain the applied loads and temperatures throughout the 100 mission cycles.

The coated columbium panel was tested at General Dynamics-Convair for a total of 100 acoustic cycles and 50 radiant heat cycles.[8] An acoustic cycle consisted of 10 sec of noise at 158 dB overall sound pressure level (OASPL), followed by 40 sec at 155 dB OASPL. The sequence of tests was 50 acoustic cycles followed by 50 thermal cycles and an additional 50 acoustic cycles. In the thermal cycles, the surface temperature was raised to 1590 K in the presence of simulated entry oxygen particle pressure. Although oxidation damage sites were observed during the test sequence, field repairs of the coating successfully prevented propagation of the oxidation damage. No significant structural damage was observed throughout the test series.

Although the tests of the full-scale models shown in Fig. 2 did not establish the useful life of the models, since structural failures did not occur, the TD-Ni-20Cr panel demonstrated a minimum life of 100 missions, and tests on the other designs were sufficient to indicate the good durability and reusability of metallic TPS.

Surface/Stream Interaction

In order to accommodate thermal growth, the surfaces of metallic TPS are generally either concave or convex corrugations. Although surface roughness effects have been studied extensively, only limited attention has been given to the more practical problems of large entry vehicles (such as the shuttle) where boundary-layer thicknesses are an order of magnitude greater than the height of the surface irregularity.[10] To assess the influence of typical TPS wavy

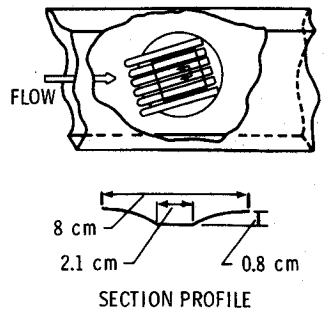

Fig. 3 Wavy surface test setpup in LaRC Unitary Plan Wind Tunnel.

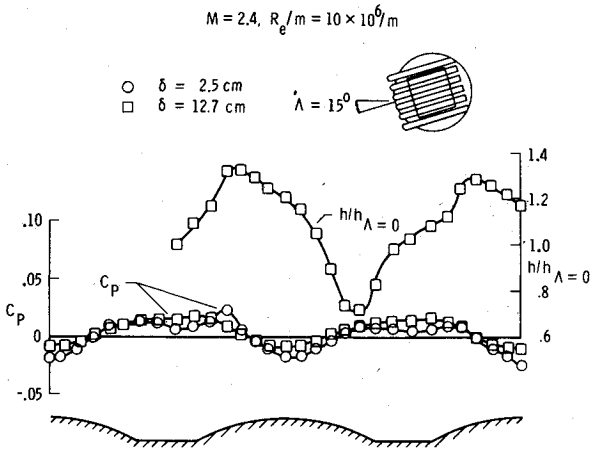

Fig. 4 Influence of a wavy surface on pressure and heating rate ($M=2.4$, $R_e/m=10\times10^6$/m).

surface configurations on drag and heating, recent tests have been conducted at Langley Research Center in a thick boundary layer representative of that over the shuttle during entry. Details of the test configuration are shown in Fig. 3, which includes a schematic of the panel mounted in the wall of the Langley Unitary Plan Wind Tunnel (UPWT). The instrumented model, outlined by the square section, is mounted in a remotely controlled turntable. The surface profile normal to the corrugations consists of circular arcs and flats. Arc close-outs and side fairings were provided to minimize the effects of the edges as the panel is yawed to the direction of flow.

A sample of data obtained on this configuration is shown in Fig. 4. The pressure coefficient C_p and heat-transfer coefficient h are plotted as functions of the location on the wavy surface. The heat-transfer coefficient is nondimensionalized by the experimentally determined value of h for a yaw angle of zero. The data are obtained in a thick turbulent boundary layer ($\delta=12.7$ cm), with the arc generators 15 deg to the direction of flow. Shown for comparison by the circle symbols is the C_p in a thin boundary layer ($\delta=2.5$ cm). (Heating rate data were not obtained in this study in the thin boundary layer.) Each of the symbols represents instrumentation locations, and the solid curves are faired through the data points. With the direction of flow at 15 deg to the corrugations, the pressure coefficients in the thick and thin boundary layers are very similar in both trend and magnitude; consequently, little difference in pressure drag is expected. The heating rate data follow the trend of the pressure coefficient, but with a shift in the peaks. For radiation equilbrium conditions, the minimum and maximum heating rate ratios shown represent a temperature differential across the corrugations of about 15% of the flat-plate value. There was no evidence of flow separation over the arcs at this yaw angle.

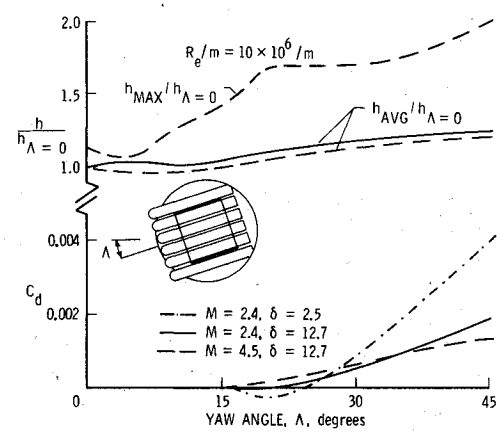

Fig. 5 Effects of wavy surface in thick turbulent boundary layer ($R_e/m=10\times10^6$/m).

Heating and drag data are shown as a function of yaw angle in Fig. 5. Data are shown for $M=2.4$ and 4.5, $R_e/m=10\times10^6$/m, and $\delta=12.7$ cm. Test conditions of $M=4.5$ and $\delta=12.7$ cm match the local conditions on the bottom centerline of the shuttle during entry.

On the heating plot, the average h and the maximum h are shown nondimensionalized by the average h when $\Lambda=0$. The average heat-transfer coefficient is reasonably constant up to $\Lambda=15$ deg and gradually increases thereafter. This increase in heating would impose a penalty on the insulation thickness. For example, at $\Lambda=45$ deg, the 20% increase in h_{av} would require about a 13% increase in insulation thickness for a shuttle entry trajectory. The maximum h shown for $M=4.5$ increases rapidly to $\Lambda=20$ deg. The heating rate ratio of 1.7 at $\Lambda=20$ deg suggests local hot regions with temperatures about 14% higher than flat-plate values. The drag coefficient is seen to be negligible for Λ up to 15 deg in both thick and thin boundary layers, and the influence of boundary-layer thickness is not apparent until the yaw angle exceeds 30 deg. At $\Lambda=45$ deg, the pressure drag for this configuration in the thick boundary layer is about half the value in the thin boundary layer. The drag coefficient of 0.002 is approximately the value of skin-friction drag on a flat plate. Although tests to date on typical metallic TPS surface configurations indicate that both drag and heating would impose some mass penalty on the TPS, these effects appear to be small in a thick boundary layer (especially where Λ is less than 20 deg), and the effects can be incorporated in TPS designs.

Cyclic Creep Prediction

Early shuttle system studies indicated that creep could become a significant factor in the design and performance of metallic TPS. The requirements of the shuttle TPS were in sharp contrast to most previous experiences in the area of creep prediction. For example, the shuttle TPS would be subjected to multiple, complex missions of combined thermal and pressure loads. Furthermore, TPS designs generally were fabricated from thin-gage material less than 1 mm thick, where the effects of oxidation on creep could be pronounced. In addition, the shuttle TPS deflection criteria limited allowable creep strains to 1%, a range where measurement and prediction capability were not well established.

By 1972, several experimental programs had been conducted to assess creep prediction capability on simple tensile specimens subjected to simulated mission cycles. Typical results from these experiments are presented in Fig. 6. Figure 6a is a representative shuttle mission temperature and pressure profile corresponding to the Earth entry mode. In Fig. 6b, the results of mission simulation tests on coated columbium sheet are summarized. The test loads were selected to produce a predicted creep strain of 1% after 100 mission cycles, as indicated by the dashed line. The maximum test temperature

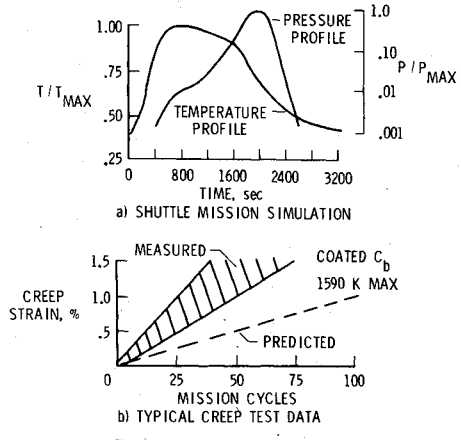

Fig. 6 Creep prediction: 1972 capability.

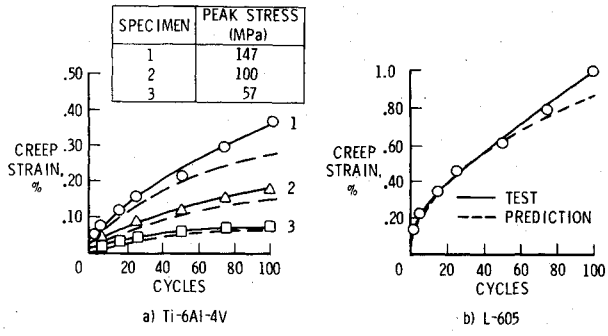

Fig. 7 Improved creep strain predictions: tensile specimens.

was 1590 K. The measured creep strains (hatched area) for different specimens exhibited considerable scatter and were consistently larger than the analytically predicted strains. Tests on other TPS materials produced similar results. Prediction capability was not good, and, more importantly, predicted strains were unconservative.

As a result of these early experiments, an extensive experimental and analytical creep investigation has been conducted on candidate TPS materials.[11] This program evaluated both the steady-state and cyclic creep behavior of four alloys in their sheet form: Ti-6Al-4V, René 41, L-605, and TD Ni-20Cr. The basic cyclic test matrix for each of the four materials included at least four temperatures and three stress levels. Each specimen was exposed to a minimum of 100 cycles. For each material, multiple regression techniques were used to assist in the development of constitutive equations to correlate the results of these simple basic cyclic experiments.

The experimental and predicted creep strains of one L-605 and three titanium specimens subjected to 100 simulated mission cycles are compared in Fig. 7. The titanium specimens (Fig. 7a) were subjected to the three maximum stress levels shown and a maximum cycle temperature of 780 K. The agreement between the test results and the predictions (which used a strain-hardening rule) is considered good, particularly at these low strain levels where measurement of creep strain is very difficult. A similar comparison for a L-605 specimen (Fig. 7b) where the maximum cycle temperature was 1200 K is considered excellent. The results of the comparisons between test and prediction for the René 41 and TD Ni-20Cr specimens did not show such good agreement. Predicted creep strains for the René 41 and TD Ni-20Cr were approximately 40 and 50% below test values, respectively. This is not considered good agreement, but it is significantly better than the 1972 prediction capability shown in Fig. 6.

To extend the prediction capability obtained from tensile specimens to more complex TPS heatshields, panel segments (6.4 × 31 cm) were tested. In order to predict creep deflections

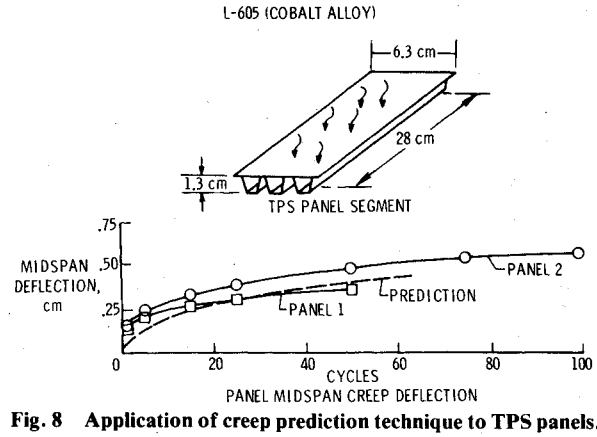

Fig. 8 Application of creep prediction technique to TPS panels.

resulting from complex stress distributions in the built-up panel, a computer program was developed which incorporates the basic cyclic correlation equations and hardening rules to calculate panel creep strains and deflections as a function of time.[11] An example of the prediction capability for corrugation-stiffened panel segments of L-605 is shown in Fig. 8. The panels were subjected to simulated shuttle mission cycles, including continuously varying temperature and pressure loads. The lower part of the figure compares the measured and predicted creep deflections of the panel midpoint as a function of the number of simulated mission cycles. The agreement between the predicted deflection and the results from two panels is considered good. For the four materials investigated, the agreement between calculated and test midpoint deflections of the panel segments was comparable to the prediction capability for the elemental specimens.

The results of the panel segment tests suggest that, if the tensile cyclic creep behavior of a material can be characterized, then creep deflection predictions can be made for thin-gage sheet structures subjected to complex cyclic thermal and bending loads. The current prediction capability, although not perfect, is considered adequate for design of metallic TPS panels that are sized by cyclic creep deformation criteria.

Thermal-Structural Design Optimization

With the increased confidence in performance of lightweight metallic TPS, a thermal-structural design process was undertaken to define and fabricate least-mass panels for subsequent service life evaluation. The TPS were designed to meet the criteria established for the space shuttle where applicable. The fruits of this optimization are indicated in Fig. 9, where unit masses of the TPS components are shown for a current state-of-the-art design and an advanced thermal-structural design. These masses are for a cobalt base material (Haynes 188), and the TPS is sized to accommodate the heat load of a shuttle entry trajectory where peak surface tem-

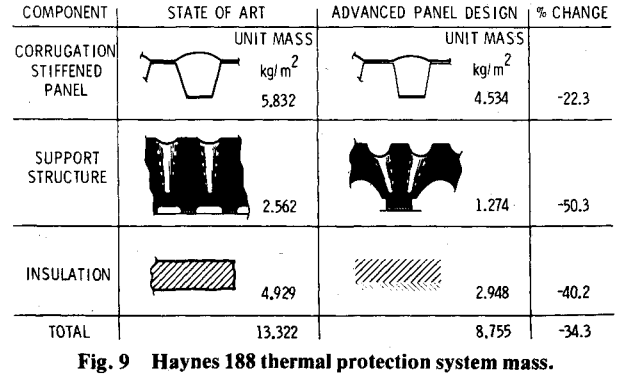

Fig. 9 Haynes 188 thermal protection system mass.

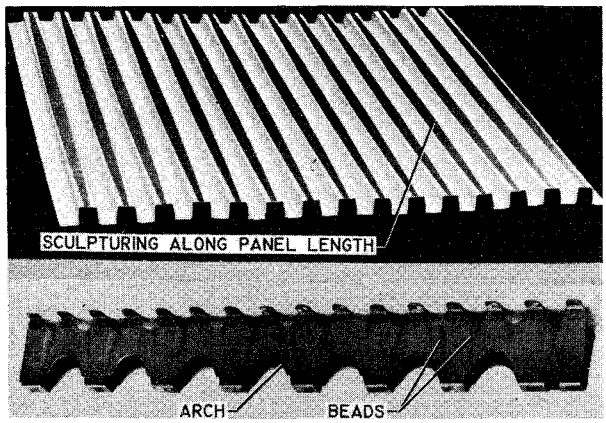

Fig. 10 Thermal-structural optimized TPS components.

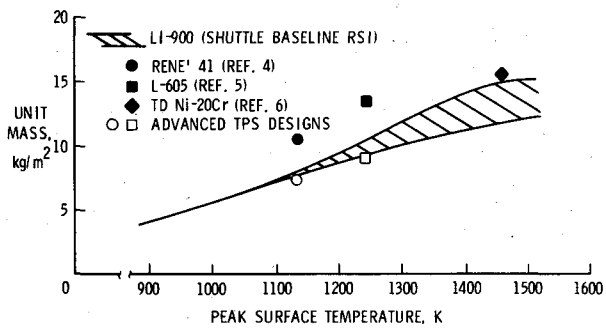

Fig. 11 Unit mass of shuttle TPS designs.

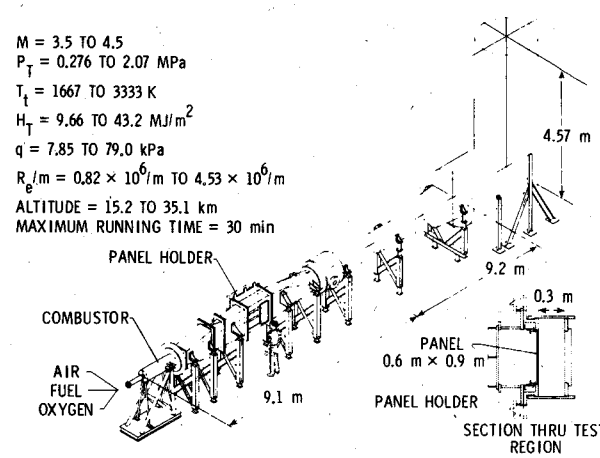

Fig. 12 Thermal protection system test facility.

perature is 1255 K. The reductions in mass of the fabricated advanced panel are 22% for the corrugation-stiffened skin, 50% for the support structure, and 40% for the insulation. These changes represent an overall 34.3% reduction in mass from the state-of-the-art design. The mass reductions in the insulation were obtained by elimination of the thin metal foil enclosure and by gradating the insulation material to maximize thermal efficiency. This design does not account for an increase in heat flux due to crossflow over the wavy surface; however, any penalty on insulation thickness was noted to be small for yaw angles less than 20 deg (see Fig. 5). The advanced design uses 57-kg/m^3 microquartz in the high-temperature region and 16-kg/m^3 TG-15 000 in the region below 700 K. The foil enclosures were used in earlier designs to prevent moisture ingress and to maintain form to the soft insulation. Recent studies have demonstrated integrity of insulation without enclosures,[6,8] and prevention of water ingress can be assured by specified ground and prelaunch procedures.

Design refinements of the corrugated stiffener and support structure are shown in Fig. 10. The corrugated stiffener has been sculptured along the panel length to minimize mass and to provide uniformity of stress. In addition, along the sidewalls, excess material has been milled chemically. The corrugated stiffener is 0.015 cm thick everywhere except the sculptured flat, which is 0.04 cm. The corrugated skin is uniformly 0.015 cm thick.

Table 1 Radiative metallic TPS test articles

Max. use temp., K	Material	Design type	Insulation, kg/m^3	Size, cm	(No. of bays)	Unit[a] mass, kg/m^2	Test environment	Comments
810	Titanium		None	102×76	(9)	5.9	...	No plans for test
1140	Rene' 41		Microquartz, 67.3	147×107	(4)	10.7	Vib., radiant heat, aerothermal flow	Ref. 4
	Rene' 41[b]		Microquartz, 56.1 TG-15 000, 16.0	76×61	(1.5)	7.3	Aerothermal flow	To be tested in NASA-LaRC-TPSTF
1260	Hastalloy-X		Microquartz, 56.1	102×51	(2)	16.1	Radiant heat, aerothermal flow	Report in progress
	L-605		Microquartz, 56.1	102×51	(2)	16.6	Radiant heat	No further tests planned
	L-605		Microquartz, 56.1	102×107	(2)	12.7	Vib., radiant heat aerothermal flow	Ref. 5
	Haynes 188[b]		Microquartz, 56.1 TG-15 000, 16.0	76×61	(1.5)	8.8	Aerothermal flow	To be tested in NASA-LaRC-TPSTF
1480	TD Ni-20Cr		Dynaflex, 96.0 Protecalor, 20.8	102×51	(2)	15.1	Radiant heat, mechanical loads	Ref. 6
	TD Ni-20Cr		Dynaflex, 96.0 Protecalor, 20.8	102×51	(2)	15.1	Aerothermal flow	To be tested in NASA-LaRC-8ft-HTST
	TD Ni-20Cr		Fiberfrax, 128	128×79	(2)	18.1	Radiant heat, mech. and acoustic loads	Ref. 7
1590	C_b		Fiberfrax, 113	122×91	(9)	22.9	Acoustic, rad. heat	Refs. 8 and 9
	C_b		Fiberfrax, 113	91×61	(3)	22.9	Aerothermal flow	To be tested in NASA-LaRC-TPSTF

[a] Includes metallic panel, supports, insulation, and attachment hardware. [b] Advanced designs.

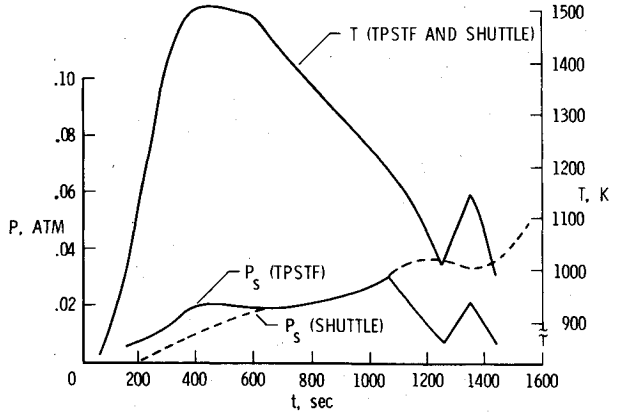

Fig. 13 Test conditions for metallic TPS in LaRC TPSTF (shuttle data at body station 0.6, trajectory 14414).

The support structure is fabricated from Haynes 188 (0.015 cm thick) and utilizes the efficiency of beads and arches to provide adequate stiffness to distribute the 20-kPa pressure load from the panel to point loads on the primary structure. The beads also accommodate thermal strain in the lateral direction, which results from a 1000 K thermal gradient over the support height. A design similar to the Haynes 188 design is being fabricated using René 41 nickel-base alloy for use temperatures to 1145 K, and mass reductions of 30% over state-of-the-art designs are projected.

Unit masses of state-of-the-art TPS hardware and advanced thermal-structural designs are shown in Fig. 11 compared with the unit mass of the shuttle RSI. The unit mass of the RSI includes the tiles, the strain isolator pad, and bonding material. The hashed region shown for the RSI mass is indicative of insulation thickness variations necessary to maintain mold line over the bottom surface of the shuttle. Although the RSI is required to prevent the primary structure temperature from exceeding 450 K, mold line fairing results in tile thicknesses both less than and greater than the design thicknesses, and primary structure temperatures may deviate from the design value by as much as 50 K. The unit masses of the metallic TPS are plotted at their corresponding maximum use temperatures. The solid symbols are the tried and proven metallic TPS listed in Table 1, and the open symbols are the advanced designs. The advanced designs are seen to be competitive with the directly bonded RSI.

Service Life Test Facility

The advanced TPS panels fabricated from René 41 and Haynes 188 will be evaluated for cyclic life characteristics in the Langley Thermal Protection System Test Facility (TPSTF). This facility is a blowdown wind tunnel that utilizes the combustion of methane, oxygen, and air to achieve test conditions representative of entry flight.[12] A sketch of the TPSTF is shown in Fig. 12. Panels up to 61×91 cm are mounted flush with the test-section wall as indicated by the inset. The range of operating conditions is listed on the figure. The channel flow is turbulent, with a surface shear of 240 Pa and a boundary-layer thickness of approximately 12.7 cm.

Typical surface temperatures and static pressures that can be imposed on the panel are shown in Fig. 13 compared with corresponding entry conditions for the shuttle at a station along the bottom centerline. Although entry surface temperature histories can be duplicated, the tunnel surface pressure, and hence shear force, is higher over most of the trajectory. The advanced TPS test panels will be subjected to a large number of such entry cycles to assess their thermal and structural characteristics, creep behavior, and joint and support efficiency. The planned test program will be the most comprehensive ever conducted on metallic TPS, since the cyclic test data will be obtained in a true aerodynamic environment with simultaneous aerodynamic heating, differential pressure, and boundary-layer acoustic loads.

Concluding Remarks

A broad-based technology program has been conducted to advance the state-of-the-art of radiative metallic thermal protection systems to the point where designers can make rational decisions on materials and configurations for future high-speed and entry vehicles. During the past five years, metallic TPS for application at use temperatures from 1145 to 1590 K have been designed, fabricated, and tested in simulated mission environments. These tests have demonstrated the durability and reusability of large flight-weight metallic TPS, and surface/stream interaction studies indicate that wavy surface drag and heat-load penalties in thick boundary layers may be acceptable for yaw angles to 20 deg. In addition, improved cyclic creep prediction techniques have increased confidence in creep-sensitive designs. Finally, advanced thermal-structural metallic TPS designs for space shuttle application are mass competitive with the shuttle RSI. In view of these results, it is concluded that the basic technology for metallic TPS is in hand, although a remaining task is to determine life characteristics for specific applications. Future studies also may address detailed problems such as TPS designs for areas of shock impingement, high-pressure gradients, and complex contours.

References

[1] "Outlook for Space," Rept. to the NASA Administration by the Outlook for Space Study Group, NASA SP-386, Jan. 1976.

[2] Henry, B.Z. and Decker, J.P., "Future Earth Orbit Transportation Systems/Technology Implications," *Astronautics and Aeronautics,* Vol. 14, Sept. 1976, pp. 18-28.

[3] Stein, B.A., Bohon, H.L., and Rummler, D.R., "An Assessment of Radiative Metallic Thermal Protection Systems for Space Shuttle," NASA TM X-2570, 1972.

[4] Deveikis, W.D., Miserentino, R., Weinstein, I., and Shideler, J.L., "Aerothermal Performance and Structural Integity of a René 41 Thermal Protection System in a Mach 6.6 Stream," NASA TN D-7943, 1975.

[5] Bohon, H.L., Sawyer, J.W., Hunt, L.R., and Weinstein, I., "Performance of Thermal Protection Systems in a Mach 7 Environment," *Journal of Spacecraft and Rockets,* Vol. 12, Dec. 1975, pp. 744-749.

[6] Eidenoff, H.L. and Rose, L., "Thermal-Structural Evaluation of TD Ni-20Cr Thermal Protection System Panels," NASA CR-132487, 1974.

[7] Johnson, R. Jr., and Killpatrick, D.H., "Evaluation of Dispersion Strengthened Nickel-Base Alloy Heat Shields For Space Shuttle Application," NASA CR-2614, March 1976.

[8] Rummler, D.R. and Black, W.E., "Evaluation of Coated Columbium for Thermal Protection Systems Application," AIAA Paper 75-187, Denver, Colo., April 1975.

[9] Black, W.E., "Evaluation of Coated Columbium Alloy Heat Shields for Space Shuttle Thermal Protection System Application," NASA CR-112119-2, 1973.

[10] Brandon, H.J. and Masek, R.V., "Measurements and Correlations of Aerodynamic Heating to Surface Corrugation Stiffened Structures in Thick Turbulent Boundary Layers," NASA CR-132503, 1975.

[11] Davis, J.W. and Cramer, B.A., "Predictions and Verification of Creep Behavior in Metallic Materials and Components for the Space Shuttle Thermal Protection System," NASA CR-2685, July 1976.

[12] Klich, G.F., "The Langley Thermal Protection System Test Facility: A Description Including Design Operating Boundaries," NASA TM X-73973, Nov. 1976.